UNCLASSIFIED

AD 423951

DEFENSE DOCUMENTATION CENTER

FOR

SCIENTIFIC AND TECHNICAL INFORMATION

CAMERON STATION, ALEXANDRIA, VIRGINIA

DAVIDSON
LABORATORY

STEVENS INSTITUTE
OF TECHNOLOGY

CASTLE POINT STATION
HOBOKEN, NEW JERSEY
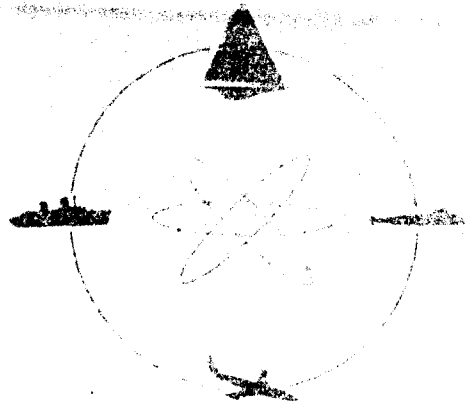
REPORT 95?

VENTILATION INCEPTION
ON A SURFACE-PIERCING DIHEDRAL HYDROFOIL
WITH PLANE-FACE WEDGE SECTION

by

Gerard Fridsma

October 1963

DAVIDSON LABORATORY

REPORT 952

October 1963

VENTILATION INCEPTION
ON A SURFACE-PIERCING DIHEDRAL HYDROFOIL
WITH PLANE-FACE WEDGE SECTION

by

Gerard Fridsma

Approved

P. Ward Brown, Chief
High-Speed Craft Division

SUMMARY

A surface-piercing, dihedral hydrofoil was tested to investigate the inception and extent of ventilation. The foil of wedge-shaped cross-section and dihedral angle of 30 degrees was shown to ventilate under a number of operating conditions when the speed, draft, and angle of attack were varied. Stable regions of fully attached and fully ventilated flow are defined by ventilation inception boundaries which are shown to depend on the speed and angle of attack and not on the depth of submergence. Expressions for the forces experienced by the foil under these stable flow conditions are derived and are shown to be in good agreement with the experimental results.

CONTENTS

NOMENCLATURE

A   aspect ratio, $A = 2(h_o/c) \cot \Gamma$

a_o sectional lift-curve slope at infinite depth, per radian

a_e effective lift-curve slope at depth, per radian

c   hydrofoil chord measured along lower surface, ft

C_D drag coefficient, $D/\frac{1}{2} \rho V^2 S$

C_L lift coefficient, $L/\frac{1}{2} \rho V^2 S$

C_L' sectional lift coefficient

C_f skin friction drag coefficient based on wetted area

D   drag force, lb

E   Jones' edge correction factor

F   depth correction factor

h   local submergence of foil cross-section below water surface, ft

h_o submergence of foil trailing edge apex below water surface, ft

K   induced drag factor

L   lift force, lb

S   horizontal projection of hydrofoil wetted area, $S = 2h_o c \cot \Gamma$, sq ft

V   forward speed, fps

α sectional angle of attack, rad

Γ dihedral angle, deg

δ wedge angle, rad

ρ density of water, 1.94 slug per cu ft

τ trim, angle between horizontal and hydrofoil lower surface, rad

INTRODUCTION

The surface-piercing, fully-ventilated hydrofoil has been under study at the Davidson Laboratory for some time, because of its potential application to high speed self-stabilizing hydrofoil craft, in order to learn more of the force characteristics of this type of foil and the flows associated with it.

In the investigations conducted by Brown[1] and Fridsma[2] on the fully vented foil, flow studies revealed the existence of ventilation inception boundaries and the occurrence of partial flow attachment to the upper surface, styled partial ventilation. Since any fully-ventilated or supercavitated hydrofoil may suffer flow attachment to the upper surface under a variety of operating conditions in steady state and under dynamic conditions, and thereby undergo marked changes in its operating characteristics, a study of ventilation inception and partial ventilation is timely.

This report presents the results of tests to determine experimentally the inception and extent of ventilation on a surface-piercing, fully-ventilated dihedral hydrofoil of plane-face wedge cross section. The parameters investigated for their effect on ventilation inception included angle of attack, immersion and speed. Force measurements and flow photographs were taken at the various test conditions during which time three flow regimes were observed: fully ventilated, fully attached flow and an intermediate partially ventilated flow regime.

It was found that the three flow regimes were distinguishable by the differing behavior of the lift characteristics. These characteristics were analyzed and theoretical relations obtained for the lift in both the stable flow states of fully ventilated and fully attached flows.

This report is one of a series prepared at the Davidson Laboratory dealing with surface-piercing fully ventilated dihedral hydrofoils. Other topics covered in this series include force and stability characteristics, behavior in a seaway and the effect of flaps. This research is being supported by the Mechanics Branch, Office of Naval Research.

MODEL AND APPARATUS

The hydrofoil model used for these tests consisted of two limbs, 14 inches long, assembled to form a V-type, surface-piercing foil of 30° dihedral and 24 in. span. The foil cross-section, which was constant along the span, was a simple wedge of 2 in. chord and 6° apex angle. In order to machine the sharp leading edge with a minimum of warping, the foil was constructed of No. 496 Starrett flat stock steel. This oil hardened, tool steel has non-deforming characteristics which make it useful for intricate work with thin sections. Nevertheless, with all the care taken in the machining process, a minute upturn of the leading edge occurred. When completed, the entire foil was given a "flash" copper plating to prevent rusting. A drawing of the model foil and a photograph is included as Fig 1.

Two vertical struts of rectangular cross-section were screwed to the ends of the foil, which in turn were fastened to a 1" x 2' spanwise aluminum member. This entire assembly was mounted on the standard Tank 3 lift-drag apparatus which is a carriage capable of measuring the total horizontal and vertical forces experienced by the foil at speed. Force measurements were obtained from dynamometers actuating linear differential transformers whose outputs were relayed to shore through overhead cables and measured with electronic null-balances.

TEST PROCEDURE

The tests were conducted in Tank 3 of the Davidson Laboratory with the foil fixed at zero roll and yaw. With the foil in the air just clear of the water surface, air tares were taken on the lift and drag balances at various speeds and trims of the foil. The air tares for the lift were found to be negligible while those for the drag were a function of the speed squared, $(D = 0.0008\ V^2)$. With the foil in the water, tests were run at draft/chord ratios of 1, 2 and 3, trims from 0° to 14° and speeds from 10 to 40 fps. Lift, drag, and speed were recorded; and polaroid pictures were taken of the flow in each case.

The test program was set up so as to define the various flow regimes: It was known that at some low trim (as yet undefined) the flow would attach to the upper surface of the foil and run in a fully attached but base vented,

flow condition. Furthermore at some high trim, the flow should separate from the leading edge and run in a fully ventilated condition. During the tests, therefore, the foil attitude was varied from low to high angles so as to determine the critical trims and how they were affected by speed and draft. The nature of the flow was determined from studies of the associated flow pictures.

RESULTS

Results from the tank testing were in the form of force measurements of the lift and drag and polaroid pictures of the flow about the foil. With this information it was possible to separate the data as to whether the flow was fully ventilated, fully attached, or partially ventilated. Tables I, II and III, present the corresponding tabulated results of the force measurements which have been corrected for air tares and put in coefficient form. In the case of borderline test conditions where it was not certain what type of flow was present, the data was assumed to lie in the unstable, partially ventilated flow regime. Occasionally there would be a test condition when the flow would remain stable and fully attached to the foil; and then during the run suddenly start to ventilate. In these cases, the data for both conditions is reported separately. All coefficients for the various flows were calculated on the basis of the horizontal projected area, $S = 2h_o c \cot \Gamma$.

The derived sectional lift characteristics for both fully attached and fully ventilated flow are plotted on Fig 2. Fully ventilated drag data are given on Fig 3, while the ventilation boundaries and a selection of flow photographs are given on Fig 5.

ANALYSIS

From an examination of the results presented in the tables and their classification into the three regimes of fully ventilated, partially ventilated, and fully attached flow, a strong correlation between the state of the flow and the lift characteristics was established.

The following description of the flow and lift changes with trim and speed is typical.
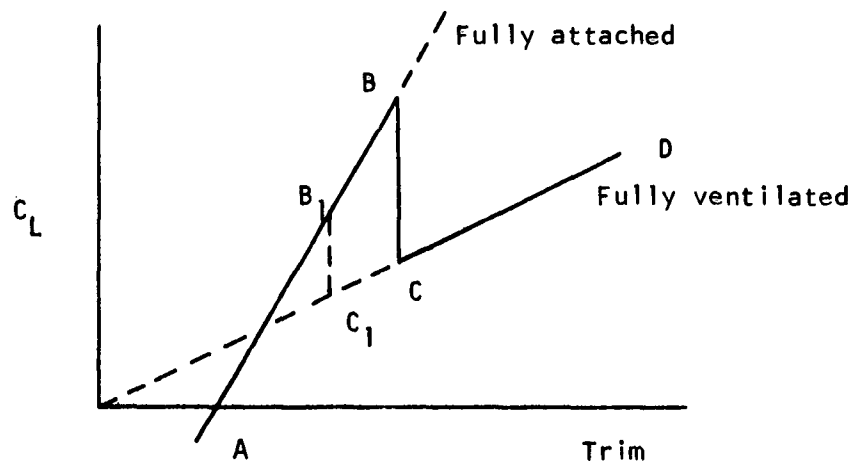
Consider the hydrofoil running at any one speed. At low trim the flow will be fully attached (though base vented) and as the trim is increased the lift increases, along the line A-B in the sketch, while the flow remains unaltered. Then at some critical trim partial ventilation of the upper surface becomes apparent and as the trim is increased further the lift drops eventually to C where observation of the foil shows it to be fully vented. Thereafter as the trim is increased the upper surface of the foil remains dry and vented to the atmosphere, and the lift again starts to increase along the line CD.

When this cycle is repeated at higher speed transition from fully attached to fully ventilated flow takes place at a smaller trim along the line B_1C_1 . Similar behavior is observed when the test is repeated at different depths of immersion.

On a surface-piercing dihedral hydrofoil, as the draft is varied the aspect ratio necessarily changes. The effect of aspect ratio on the lift of a three-dimensional foil may be eliminated by reducing the results to their two-dimensional or sectional equivalent. Because of the strong correlation between the lift and ventilation inception, a similar procedure should remove the effect of aspect ratio from the inception characteristics.

The procedure for elimination of the aspect ratio effects from the force characteristics of a fully ventilated foil has been given by Brown[1], however a similar procedure for foils in fully attached flow is wanting. The following is a generalization of the technique for eliminating aspect ratio effects which applies to foils in both fully ventilated and fully attached flow.

General Lift Expression

The two-dimensional or sectional lift, denoted by a prime, of a hydro-foil may generally be written in the form:

$$C_L' = a_o(\alpha - \alpha_o) \tag{1}$$

The sectional lift-curve slope, a_o , and the sectional zero-lift angle, α_o , both depending on the flow conditions.

When this section is incorporated as part of a finite aspect ratio dihedral foil at finite draft a number of modifications have to be made to Eq 1. Due to the finite aspect ratio a downwash velocity is induced behind the foil so that the effective angle of attack is reduced by the downwash angle, ϵ , where generally:

$$\epsilon = K\, C_L/\pi A$$

and K is called the induced drag factor. A further effect associated with aspect ratio is that at each section, due to the finite perimeter of the foil, less circulation is needed to move the rear stagnation point to the trailing edge. Thus, the lift curve slope is reduced by the Jones[4] edge correction factor, E , and becomes a_o/E , (where E > 1).

Finite draft further modifies the lift expression. The change in circulation is accounted for by a free surface factor, F , so that the lift curve slope becomes $a_o F$: this factor may be either greater or less than unity depending on the flow conditions. There is, however, no additional change in downwash due to finite depth alone. In the case of a fully submerged foil the downwash is affected by finite draft, as well as by finite aspect ratio. This however is not the case for a surface-piercing dihedral foil[6], and no further modification of the above expression for downwash, to account for finite draft, is called for. This amounts to saying that the induced drag factor, K , is independent of draft.

Conversely dihedral will affect the downwash. Further the trim of a dihedral foil and the sectional angle of attack are related[1] by $\alpha = \tau \cos \Gamma$.

With the ¿icated modifications incorporated in Eq 1, the lift of a finite aspect ratio surface-piercing dihedral foil takes the form:

$$C_L = a_o(F/E) \cos \Gamma(\tau - \tau_o - \epsilon)$$

or $\quad C_L = C'_L \dfrac{(F/E)\pi A}{\pi A + (F/E)K\, a_o\, \cos \Gamma}$ $\qquad\qquad$ (2)

where $\qquad C'_L = a_o \cos \Gamma(\tau - \tau_o)$

Thus using Eq 2 the equivalent two-dimensional lift may be found from the three-dimensional data. The particular values to be used for the lift-curve slope and correction factors depend on the flow conditions. The values for the two stable flow regimes -- fully ventilated and fully attached -- are discussed separately below.

Fully Ventilated Flow
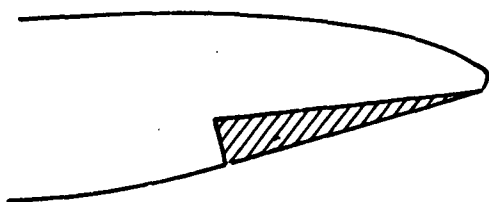
The flow about the wedge section foil is termed fully ventilated when free streamlines form at the leading and trailing edges, bounding a cavity over the top of the foil that extends some distance downstream and is vented to the atmosphere.

For this flow condition the theoretical sectional lift-curve slope at infinite depth is $a_o = \pi/2$, Parkin[3].

Theoretical values of the factors K , E and F are not available, however empirical values of these factors have been obtained by Brown[1] from experimental measurements of the forces on a family of surface-piercing fully ventilated dihedral hydrofoils. These values are $E = F = 1$ and $K = \sec \beta$, and have been confirmed in further experiments by Fridsma[2]. Substituting these values in Eq 2 the two-dimensional lift is given in terms of the measured lift by

$$C'_L = C_L\ (2A + 1)/2A = \frac{\pi}{2} \cos \Gamma(\tau - \tau_o) \qquad\qquad (3)$$

Using the lift data for fully ventilated flow given in Table I, C'_L was formed as indicated by Eq 3 and is shown plotted against $\tau \cos \Gamma$ in Fig 2, lower line. The boxes represent 37 data points, taken at various speeds and aspect ratios (drafts), the height of the boxes showing the range of variation while the symbol indicates the mean value. A good collapse is obtained

about a line having a slope of $\pi/2$ with a zero lift angle of $\tau_o \cos \Gamma = 0.55°$. The existence of a finite zero lift angle on a nominally flat-faced foil is accounted for by a minute upturn of a few thousandths of an inch at the leading edge.

The drag is shown plotted in the previously developed form[2] for fully ventilated foils:

$$C_D \cos \tau = C_L \sin \tau + C_f \sec \Gamma$$

on Fig 3. The ordinate intercept varies but little over the speed range of 15 to 40 fps and a mean value of $C_f \sec \Gamma = 0.0065$ was used. Data taken at 10 fps is not included on this plot since drag data at this low speed was thought to be unreliable. The remaining data are shown to cluster closely about the theoretical line.

Fully Attached Flows (Base Vented)
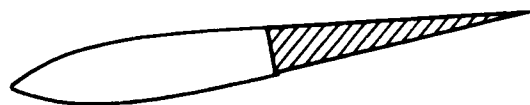
The flow is called fully attached when the whole of the upper surface, as well as the lower surface, is completely wetted by the flow. For the wedge section used in this investigation the flow separates from the base of the foil, forming a cavity which is again vented to the atmosphere. Parkin[3] has shown that the section lift-curve slope for this condition, at infinite depth, is 2π .

Because of the similarities between the fully attached, base vented, flow and the flow about an airfoil, a surface-piercing dihedral hydrofoil may be likened to an airplane wing. Making use of this analogy theoretical expressions for the factors E , F and K have been developed from wing theory.

Edge Correction Factor E Jones[4] pointed out that an elemental strip of a finite wing should require less circulation to meet the Kutta condition than the same element in an infinite wing. For an elliptical planform wing he showed theoretically that the circulation, and hence the lift-curve slope, was reduced by a factor E , where:

$$E = \text{semi-perimeter/span}$$

Assuming that the same rule applies to a rectangular planform wing, E may
be expressed in terms of the aspect ratio:

$$E = (A + 1)/A \qquad\qquad\qquad (4)$$

Depth Correction Factor F   As an approximate means of determining the
effect of depth on the circulation about a two-dimensional foil beneath a free
surface, Wadlin[5] represented the foil by a single vortex at the center of
pressure, with a symmetrical image above the waterline to satisfy the free
surface condition. This procedure is similar to that used in biplane theory
and stems from the fact that the boundary value problems for a foil moving at
high speed beneath a free surface and for a two-dimensional biplane are simi-
lar. An exact solution to this boundary value problem was obtained by Glauert,
and comparison shows that the approximate procedure gives valid results, par-
ticularly for depth/chord ratios greater than 0.5. Wadlin's expression for
the sectional lift-curve slope at finite depth to that at infinite depth is:

$$\frac{a_e}{a_o} = \frac{(4h/c)^2 + 1}{(4h/c)^2 + 2} \qquad\qquad (5)$$

Since the draft varies across the span of a surface-piercing dihedral foil,
from zero at the tips to h_o at the apex, the value of the factor F is
found by averaging Eq 5 across the span:

$$F = \frac{\bar{a}_e}{a_o} = \frac{1}{h_o} \int_0^{h_o} \frac{a_e}{a_o} \, dh$$

therefore $$F = 1 - \frac{\text{arc tan } 2\sqrt{2}\ (h_o/c)}{4\sqrt{2}\ (h_o/c)} \qquad\qquad (6)$$

The factor F can also be expressed in terms of the aspect ratio since
$A = 2(h_o/c) \cot \Gamma$. On substituting for (h_o/c) in Eq 6, it is found that
a good approximation for Eq 6 is:

$$F = 1.78\ A \tan \Gamma/(1 + 1.78\ A \tan \Gamma)\ , \qquad A \tan \Gamma > 0.7 \qquad (7)$$

For the present tests in which the dihedral angle $\Gamma = 30^{\circ}$, Eq 7 yields

$$F = A/(1 + A)\ , \qquad\qquad\qquad A > 1.2 \qquad (8)$$

The fact that, for these tests, F = 1/E is coincidental.

<u>Induced Drag Factor K</u>   The minimum induced drag of any wing system, such as monoplane, biplane, or boxplane, can be calculated by making use of the fact that minimum induced drag is attained when the downwash velocity is constant throughout the wake. Such calculations are standard in the litera- ture of wing theory, and their practical value is due to the fact that the induced drag is insensitive to quite large departures of the lift distribu- tion from that which gives constant downwash in the wake. Making use of this technique from wing theory, Brown[6] has calculated the minimum induced drag of a surface piercing foil and finds a theoretical expression for K which may be approximated by:

$$K = 2(1 - \Gamma^{o}/75) \qquad\qquad \Gamma > 60^{o} \tag{9}$$

$$= 1.2 \quad \text{for} \quad \Gamma = 30^{o}$$

Substituting $a_o = 2\pi$, and for E and F the expressions given by Eq 4 and 8, into Eq 2 the two-dimensional lift of the fully wetted surface- piercing dihedral foil is given in terms of the measured lift by:

$$C_L' = C_L \left[(\frac{1+A}{A})^2 + \frac{2 K \cos \Gamma}{A} \right] 2\pi \cos \Gamma (\tau - \tau_o) \tag{10}$$

For a foil with 30° dihedral, since K = 1.2 , Eq 10 reduces to

$$C_L' = C_L \frac{A + 4.08 + 1/A}{A} = 2\pi \cos \Gamma (\tau - \tau_o) \tag{11}$$

which is a form for the fully wetted foil comparable to that given by Eq 3 for the fully vented foil.

Using the lift data for fully attached, base vented, flow given in Table III the sectional lift coefficient was formed using Eq 11 and is shown plotted on Fig 2, upper line, against $\tau \cos \Gamma$. The theoretical slope of 2π is confirmed by the data, but depth effect is not completely eliminated since the zero lift angle increases somewhat with increasing depth. For a dihedral foil with wedge section at infinite depth it would be expected that the zero lift trim, which is referred to the lower face of the wedge, would be given by $\tau_o \cos \Gamma = \delta/2$, where δ is the wedge apex angle. The observed varia- tion of the zero lift angle with a depth parameter is shown on Fig 4. The theory of a two-dimensional base vented foil at finite depth has not been developed, but a tentative extrapolation to $\tau_o = 0$ at h/c = 0 (the planing condition) is shown.

Fully attached flow can only be maintained at small trims and speeds where the drag is also small. It is considered that the drag data, obtained as an incidental to these tests, is not sufficiently reliable to warrant its being plotted.

Ventilation Characteristics

When a surface-piercing, dihedral hydrofoil is operating with the flow fully attached to the foil upper surface, ventilation will occur if the angle of attack or speed are made sufficiently high. Ventilation begins when the pressures on the upper surface are below atmospheric. Local separation of the flow will result, starting from the free surface and an air cavity will form, gradually working its way down the foil. Because of the sharp leading edge on the foil section, separation normally starts here. When sufficient air has been introduced at higher trims and speeds, complete separation will occur and the foil will operate in fully-ventilated flow with the upper surface entirely open to the atmosphere. The transition from fully attached to fully ventilated flow takes many interesting forms (see Fig 5). Sometimes the change is very sudden, while at other times the change is gradual. The flow itself may look completely different; sometimes appearing as ventilation of only one or part of a limb of the foil, or appearing as an alternate attacned and separated flow.

The ventilation characteristics were analyzed by constructing auxiliary plots such as that of lift against speed for constant trim shown in the following sketch

Froude No. $V/\sqrt{gc}$
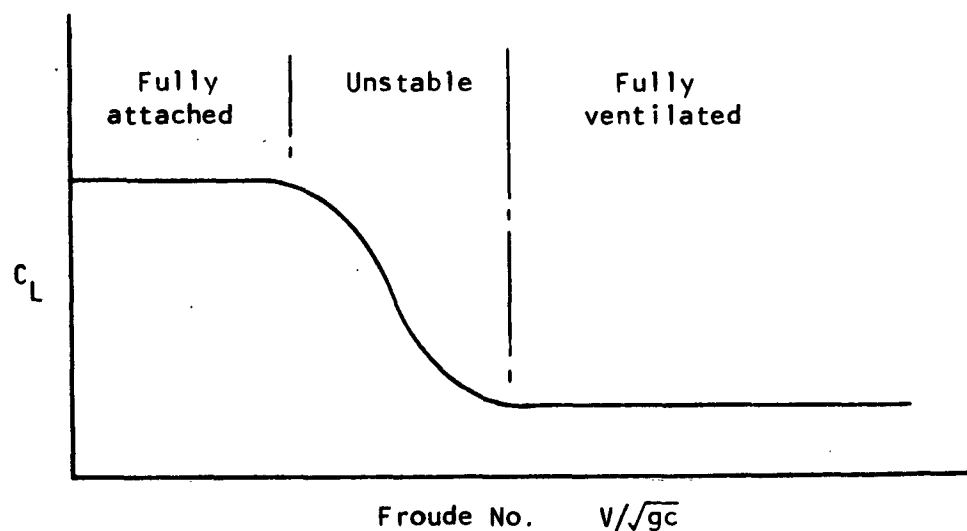
The Froude number based on the hydrofoil chord was used in an attempt to remove scale effects from the data. The flow regimes indicated on the sketch were verified by a study of the flow photographs. From these plots the speeds marking the boundaries of the different flow regimes were found and plotted as functions of trim in Fig 5 with corresponding flow photographs. These same boundaries are shown in combination with the lift characteristics in Fig 6.

DISCUSSION

The results of the force measurements on the fully ventilated, surface-piercing dihedral foil confirm previous experiments and analyses[1,2] and do not call for comment.

The analysis developed herein of the lift under fully attached, base vented, flow conditions, while successfully rationalizing the data, differs in one particular from that for fully ventilated flow. In the case of fully ventilated flow on surface-piercing foils it was found to be unnecessary to take separate account of the depth effect on lift[1], which was included in the aspect ratio correction. On the other hand for the surface-piercing foil with attached flow the depth effect is accounted for explicitly with a separate adjustment for aspect ratio effect. It should be noted that it is still possible to treat these two effects as one combined effect in the case of the fully wetted foil, however a large value of the induced drag factor, K, results if this is done. The Jones edge correction could also be suppressed at the cost of a further increase in the induced drag factor. These difficulties could only be resolved by more extensive force measurements of foils in fully attached flow, probably including two-dimensional tests, but were not undertaken in this study which was primarily concerned with ventilation.

The fact that the lift characteristics for fully attached flow show a variation in the zero lift angle with depth emphasizes the need for a theoretical study, and further experimental study, of fully wetted foils beneath a free surface.

A theoretical analysis of ventilation inception has not been attempted in this investigation which is intended primarily to provide information on the inception boundaries. That the phenomenon of ventilation is a complex one may be stressed by consideration of one aspect. The theoretical study of

hydrofoils has been confined almost exclusively to foils moving in a perfect fluid, but for a wedge section foil with sharp leading edge in a perfect fluid ventilation or cavitation should be present unless the stagnation point is at the leading edge. The fact that ventilation does not start as soon as the stagnation point moves off the leading edge may probably be attributed to the influence of viscosity, furthermore the fact that the inception boundaries are speed dependent suggests that the influence of gravity cannot be neglected.

The ventilation boundaries shown in Fig 6 are functions of speed and trim only, and, for the range of depths covered in this investigation -- one to three chords at the foil apex -- are independent of depth. From a study of Fig 6 it appears that the flow adjusts, if the speed is high enough, to give the minimum lift. As shown in Fig 6 the fully attached and fully venti- lated lift curves intersect, to the left of this intersection the flow was always fully attached no matter how high the speed, while to the right fully ventilated flow could always be achieved by sufficient increase of speed. The two lift curves intersect at approximately $\tau \cos \Gamma = 3^{\circ}$ where, for fully attached flow, the stagnation point would be at the leading edge and it may be noted that the trim boundary for fully attached flow tends towards this same angle as the speed increases.

The combination of the ventilation boundaries with the lift character- istics on Fig 6 summarizes the behavior of the foil, and may be used as a design chart. As an example, the critical trims at a Froude number of 10 are shown projected up onto the lift curves so as to define the stable range of operation for this speed.

CONCLUSIONS

A surface-piercing, dihedral hydrofoil was tested to investigate the inception and extent of ventilation. The foil of wedge-shaped cross-section and dihedral angle of 30 degrees was shown to ventilate under a number of operating conditions as the speed, draft, and angle of attack were varied. Stable regions of fully attached and fully ventilated flow were defined by ventilation inception boundaries which were shown to depend strongly on the speed and angle of attack, but not on the depth of submergence.

The forces experienced by the foil under these stable flow conditions can be given analytically and are generally in good agreement with the

experimental results. Expressions for the lift and drag forces in fully ventilated flow, previously developed by Brown[1] and Fridsma[2], are:

$$C_L = \pi/2 \cos \Gamma(\tau - \tau_o) \frac{2A}{1+2A} \qquad\qquad \tau_o = 0.63^o$$

$$C_D \cos \tau = C_L \sin \tau + C_f \sec \Gamma$$

An expression for lift under fully attached but base ventilated flow is derived herein, utilizing the same techniques as Brown, but incorporating separate corrections for depth and edge effects. The lift formula for fully attached flow is:

$$C_L = 2\pi \cos \Gamma(\tau - \tau_o) \frac{A}{1/A + 4.08 + A}$$

The no-lift angle in the above expression increases with draft tending toward half the wedge apex angle at infinite depth.

The ventilation characteristics are shown in combination with the lift characteristics to form a chart which should be useful for design purposes.

REFERENCES

1. Brown, P. Ward: "The Force Characteristics of Surface-Piercing Fully Ventilated Hydrofoils"
    DL Report 698, October 1958.

2. Fridsma, G.: "Force and Moment Characteristics of a Surface-Piercing, Fully Ventilated, Dihedral Hydrofoil"
    DL Report 795, November 1960.

3. Parkin, Blaine R.: "Linearized Theory of Cavity Flow in Two Dimensions"
    The Rand Corporation, P-1745, July 1959.

4. Jones, Robert T.: "Correction of the Lifting-line Theory for the Effect of the Chord"
    NACA TN No. 617, 1941.

5. Wadlin, K.L., Fontana, R.E., and Shuford, C.L., Jr.: "The Effect of End Plates, End Struts, and Depth of Submergence on the Characteristics of a Hydrofoil"
    NACA RM L51B13, 1951. CONFIDENTIAL

6. Brown, P. Ward: "On the Minimum Induced Drag of a Diamond Foil"
    Unpublished DL note, 1958.

7. Glauert, H.: "The Elements of Aerofoil and Airscrew Theory"
    The MacMillan Co., New York, 1944.

TABLE I

FORCE DATA - FULLY VENTILATED

Trim τ, deg	Draft h_o, in.	Lift L, lb	Drag D, lb	Speed V, fps	C_L	C_D
5.0	2.0	13.40	2.17	41.40	.0838	.0136
	2.0	13.30	2.26	41.46	.0829	.0141
5.5	2.0	-	2.60	41.39	-	.0163
	4.0	-	5.37	41.32	-	.0168
6.0	2.0	16.05	3.10	41.36	.1006	.0194
	4.0	-	6.30	41.32	-	.0198
	4.0	37.05	6.25	41.29	.1164	.0196
	6.0	44.29	7.37	35.97	.1222	.0203
7.0	4.0	10.68	1.68	20.28	.1391	.0219
	4.0	6.45	1.12	15.12	.1511	.0262
	4.0	11.10	2.05	20.29	.1444	.0267
	4.0	-	3.20	25.91	-	.0255
	4.0	17.50	3.20	25.64	.1426	.0261
	4.0	-	3.90	29.17	-	.0245
	4.0	24.30	4.48	30.38	.1410	,0260
	4.0	33.90	6.32	35.95	.1405	.0262
	4.0	44.00	7.74	41.29	.1382	.0243
	6.0	17.19	2.80	20.28	.1492	.0243
	6.0	52.04	8.76	26.02	.1433	.0241
8.0	2.0	5.60	0.98	20.28	.1459	.0255
	2.0	1.44	-	10.02	.1537	-
	2.0	23.12	4.26	41.39	.1447	.0266
	4.0	12.47	2.15	20.34	.1614	.0278
	4.0	12.34	2.23	20.26	.1610	.0291
	4.0	12.88	2.53	20.28	.1677	.0329
	4.0	12.94	2.43	20.29	.1684	.0316
	4.0	12.48	2.30	20.22	.1635	.0301
	4.0	50.40	9.50	40.98	.1608	.0303
	6.0	-	3.68	20.35	-	.0318
	6.0	-	3.68	20.35	-	.0318
	6.0	19.56	3.68	20.33	.1691	.0318
	6.0	60.11	11.22	35.92	.1664	.0311
9.0	4.0	14.00	2.63	20.28	.1823	.0343
	4.0	-	11.60	41.32	-	.0364
	4.0	57.95	11.80	41.29	.1821	.0371
10.0	4.0	4.15	0.72	10.03	.2210	.0383
	4.0	4.40	0.74	10.10	.2310	.0388
	4.0	15.24	3.16	20.26	.1989	.0412
	6.0	23.96	5.14	20.26	.2085	.0447

TABLE I (continued)

Trim τ, deg	Draft h_o, in.	Lift L, lb	Drag D, lb	Speed V, fps	c_L	c_D
11.0	4.0	4.59	0.92	10.08	.2420	.0485
12.0	4.0	5.00	1.12	10.09	.2630	.0589
	4.0	18.79	4.62	20.27	.2449	.0602
	4.0	18.50	4.38	20.22	.2424	.0574
14.0	4.0	5.70	1.42	10.06	.3017	.0752
	4.0	22.40	-	20.19	.2929	-

TABLE II

FORCE DATA - PARTIALLY VENTILATED

Trim τ, deg	Draft h_o, in.	Lift L, lb	Drag D, lb	Speed V, fps	c_L	c_D
4.0	2.0	10.25	2.10	41.43	.0640	.0131
	2.0	5.90	1.38	30.19	.0694	.0162
	4.0	-	3.57	34.79	-	.0158
	4.0	-	4.90	41.25	-	.0154
	4.0	-	4.70	41.29	-	.0148
	4.0	24.80	4.76	41.29	.0779	.0150
	6.0	21.85	5.27	34.82	.0644	.0155
4.5	2.0	3.95	0.38	20.16	.1042	.0100
	2.0	3.50	0.38	20.16	.0923	.0100
	4.0	7.15	1.06	20.29	.0930	.0138
	4.0	32.70	5.20	41.43	.1020	.0162
5.0	2.0	3.70	0.33	20.29	.0963	.0086
	4.0	8.54	1.24	20.27	.1113	.0162
	4.0	-	1.48	20.31	-	.0192
	4.0	9.32	1.53	20.24	.1218	.0200
	4.0	35.17	5.16	41.25	.1107	.0162
	6.0	2.87	1.04	9.96	.1033	.0374
	6.0	13.05	2.21	20.25	.1137	.0193
	6.0	42.98	6.43	35.97	.1186	.0177
5.5	4.0	9.22	1.18	20.28	.1201	.0154
	4.0	-	5.70	41.32	-	.0179
6.0	2.0	1.11	-	10.04	.1180	-
	2.0	4.25	0.54	20.28	.1108	.0141
	4.0	10.60	1.72	20.36	.1370	.0222
	4.0	11.25	1.45	20.26	.1468	.0189
	4.0	11.05	1.41	20.32	.1433	.0183
	4.0	10.50	1.48	20.33	.1361	.0192
	4.0	9.70	1.78	20.24	.1268	.0233
	6.0	-	2.61	19.99	-	.0233
	6.0	15.71	2.68	19.96	.1408	.0240
7.0	2.0	1.50	-	10.10	.1576	-
	2.0	1.50	-	10.08	.1582	-
	2.0	1.32	-	10.10	.1387	-
	4.0	3.71	0.47	10.02	.1980	.0251
	4.0	3.50	0.75	10.14	.1824	.0391
	4.0	3.12	0.77	10.10	.1639	.0404
	4.0	3.70	0.82	10.07	.1955	.0433
	6.0	6.50	1.49	9.98	.2331	.0534
8.0	2.0	1.53	-	10.02	.1633	-
	4.0	4.42	0.62	10.09	.2325	.0326
	4.0	3.80	0.62	10.09	.1999	.0326
	6.0	6.71	1.52	10.05	.2373	.0537

TABLE II (continued)

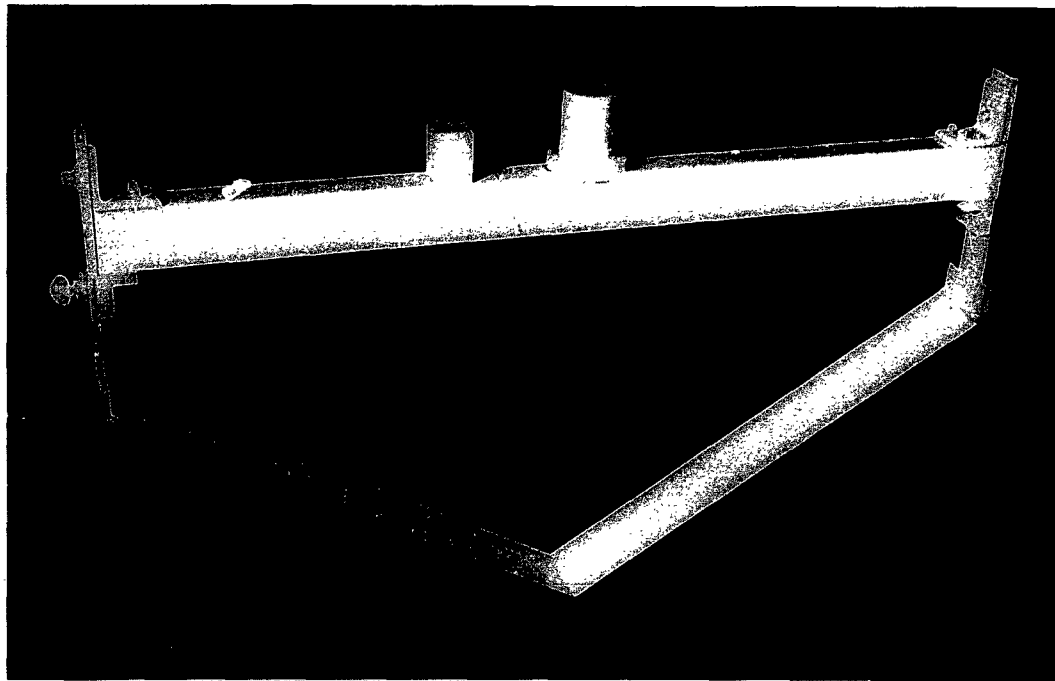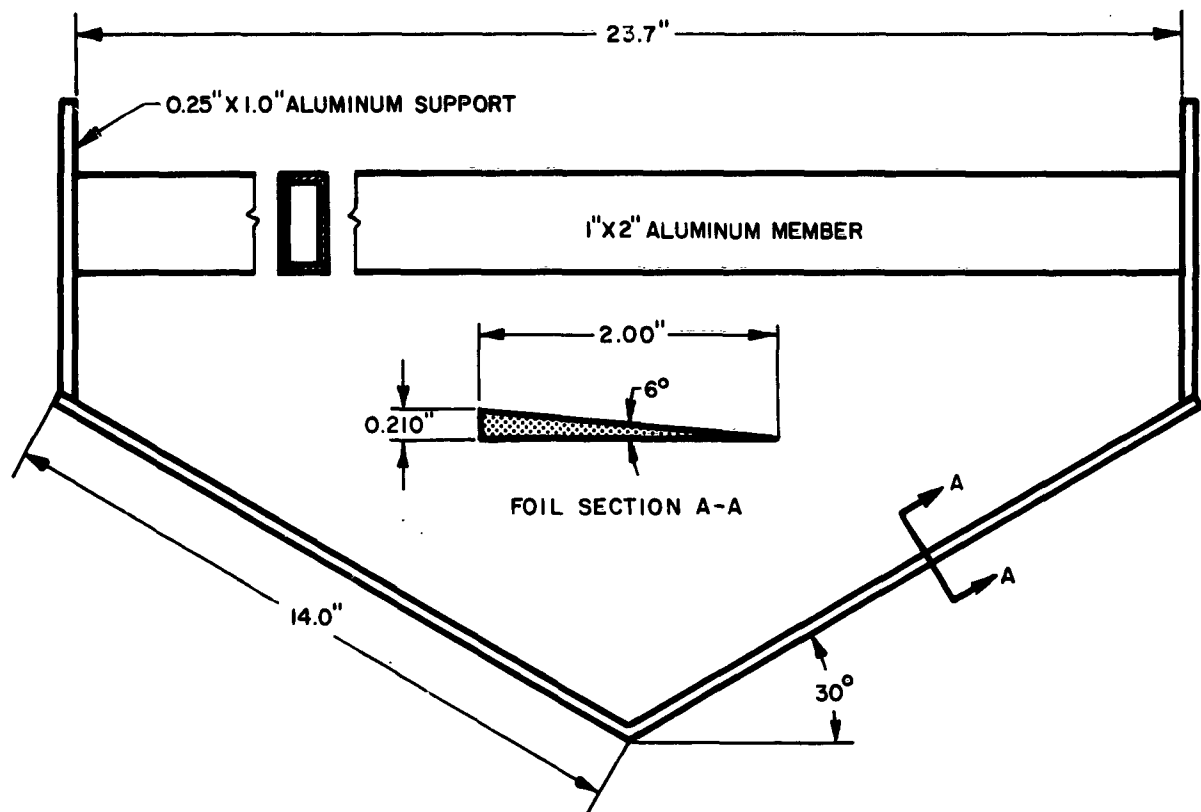| Trim τ, deg	Draft h_o, in.	Lift L, lb	Drag D, lb	Speed V, fps	C_L	C_D
8.5	4.0	4.00	0.56	10.02	.2134	.0299
9.0	4.0	5.08	0.57	10.02	.2711	.0304
	4.0	4.04	0.57	10.02	.2156	.0304
9.5	4.0	4.10	0.63	10.02	.2188	.0336
10.0	4.0	5.85	0.87	10.10	.3071	.0457
	6.0	7.12	1.90	9.98	.2553	.0681

TABLE III

FORCE DATA - FULLY ATTACHED

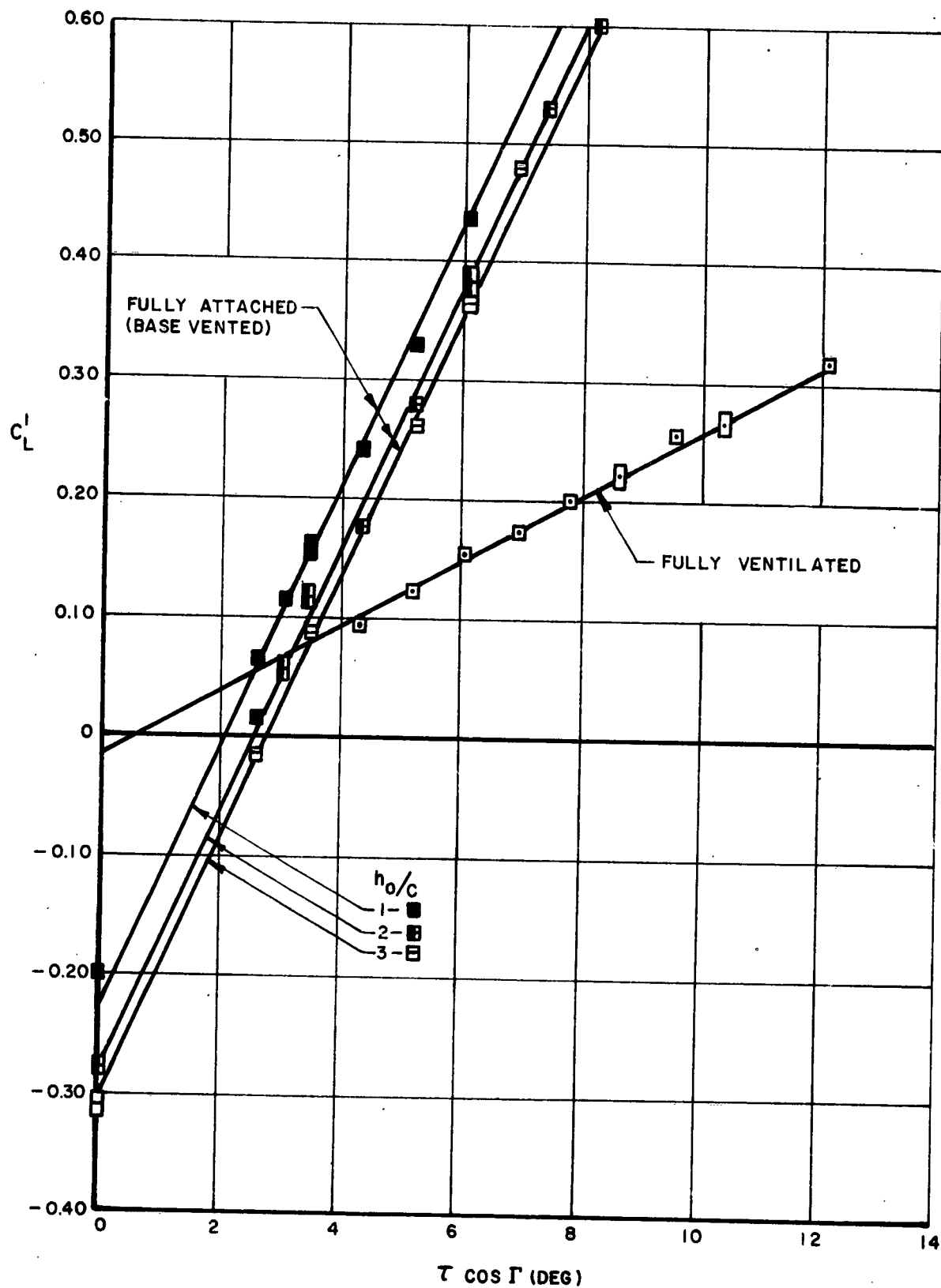| Trim τ, deg	Draft h_o, in.	Lift L, lb	Drag D, lb	Speed V, fps	C_L	C_D
0	2.0	- .80	0.22	10.00	-.0857	.0236
	2.0	-1.86	0.51	15.03	-.0853	.0242
	2.0	-3.12	0.73	19.83	-.0850	.0199
	2.0	-5.37	1.20	25.54	-.0882	.0197
	4.0	-3.28	0.52	10.05	-.1739	.0276
	4.0	-7.00	1.07	15.00	-.1666	.0255
	4.0	-	1.83	19.90	-	.0248
	4.0	-20.00	2.87	25.56	-.1639	.0235
	4.0	-29.00	4.28	30.18	-.1706	.0252
	6.0	-6.05	1.04	10.03	-.2148	.0369
	6.0	-13.00	1.92	14.88	-.2097	.0310
	6.0	-22.95	3.18	19.83	-.2084	.0289
	6.0	-	5.00	25.55	-	.0274
	6.0	-39.80	5.00	25.54	-.2180	.0274
	6.0	-	6.28	28.47	-	.0277
	6.0	-46.40	5.59	27.26	-.2230	.0269
2.0	4.0	-	1.23	20.30	-	.0160
	4.0	-	1.11	20.29	-	.0144
	4.0	-	1.29	20.29	-	.0168
3.0	2.0	1.15	-	20.25	.0301	-
	2.0	-	2.15	41.32	-	.0135
	2.0	-	1.84	41.36	-	.0115
	2.0	4.70	2.00	41.36	.0294	.0125
	2.0	4.78	1.90	41.36	.0299	.0119
	4.0	0.80	0.96	20.32	.0104	.0125
	4.0	0.90	0.88	20.30	.0117	.0114
	4.0	-	4.80	41.25	-	.0151
	4.0	-	4.80	41.25	-	.0151
	4.0	-	4.70	41.25	-	.0148
	4.0	3.05	4.40	41.25	.0096	.0139
	6.0	-0.51	1.08	9.99	-.0183	.0387
	6.0	-0.82	2.08	20.38	-.0071	.0179
	6.0	-3.02	5.62	36.00	-.0083	.0155
3.5	2.0	1.95	-	20.27	.0509	-
	4.0	0.40	-	9.43	.0241	-
	4.0	2.95	0.93	20.32	.0383	.0121
	4.0	13.80	4.59	41.22	.0435	.0145
4.0	2.0	1.40	-	15.10	.0658	-
	2.0	2.50	0.48	19.94	.0674	.0129
	2.0	2.50	0.48	19.98	.0671	.0129
	2.0	2.85	0.43	20.33	.0739	.0112
	2.0	4.40	1.40	25.69	.0715	.0227
	2.0	4.25	1.00	25.67	.0691	.0162

TABLE III (continued)

Trim τ, deg	Draft h_o, in.	Lift L, lb	Drag D, lb	Speed V, fps	c_L	c_D
4.0	4.0	-	0.82	15.17	-	.0191
	4.0	-	0.82	15.10	-	.0193
	4.0	2.55	0.82	15.11	.0598	.0192
	4.0	4.87	1.20	20.33	.0631	.0156
	4.0	4.95	1.01	20.34	.0641	.0131
	4.0	5.51	1.18	20.28	.0718	.0154
	4.0	5.40	1.41	19.93	.0728	.0190
	4.0	5.34	1.33	19.96	.0718	.0179
	4.0	5.50	1.43	19.94	.0741	.0193
	4.0	5.40	1.73	19.98	.0724	.0232
	4.0	5.32	1.73	19.99	.0713	.0232
	4.0	4.90	1.33	19.89	.0663	.0180
	4.0	9.55	1.90	25.77	.0770	.0153
	4.0	9.50	1.90	25.71	.0770	.0154
	4.0	8.90	2.00	25.59	.0728	.0164
	4.0	12.80	3.01	30.25	.0749	.0176
	6.0	1.65	0.72	10.14	.0573	.0250
	6.0	1.60	0.82	10.14	.0556	.0285
	6.0	1.65	0.90	10.02	.0587	.0320
	6.0	3.90	1.37	15.07	.0613	.0215
	6.0	3.80	1.30	15.04	.0600	.0205
	6.0	-	1.98	19.76	-	.0181
	6.0	6.85	2.10	19.82	.0623	.0191
	6.0	12.55	3.25	25.65	.0681	.0176
	6.0	11.08	3.20	25.50	.0608	.0176
	6.0	16.58	4.18	30.08	.0655	.0165
5.0	2.0	1.00	-	10.08	.1055	-
	4.0	1.98	0.32	9.99	.1063	.0172
6.0	2.0	1.35	-	10.06	.1430	-
	4.0	3.20	0.37	10.03	.1704	.0197
	6.0	5.35	1.32	10.17	.1848	.0456
	6.0	20.28	2.68	19.96	.1817	.0240
7.0	2.0	1.80	-	10.08	.1899	-
	4.0	4.20	0.47	10.02	.2240	.0251
	4.0	4.50	0.77	10.10	.2390	.0404
	4.0	3.72	0.80	9.98	.2000	.0430
	6.0	7.15	1.49	9.98	.2564	.0534
8.0	6.0	9.45	1.52	10.05	.3342	.0537
8.5	4.0	6.01	0.71	10.02	.3207	.0379
9.5	4.0	6.87	0.84	10.02	.3666	.0448

HYDROFOIL MODEL

23.7"

0.25"X1.0"ALUMINUM SUPPORT

1"X2" ALUMINUM MEMBER

2.00"

6°

0.210"

FOIL SECTION A-A

A

A

14.0"

30°

FIG 2

LIFT CHARACTERISTICS

DRAG CHARACTERISTICS (FULLY VENTILATED)
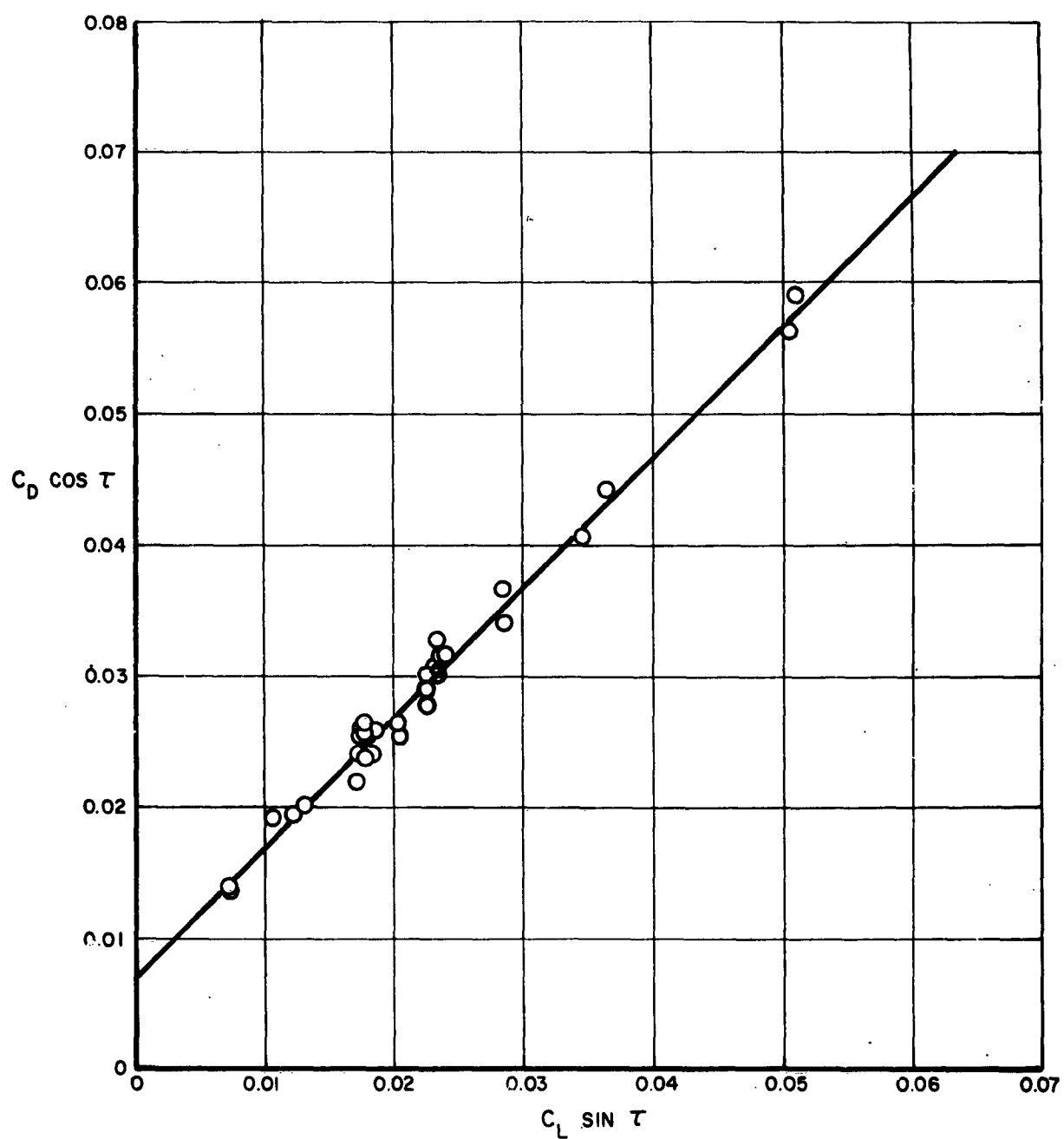
SHIFT IN ZERO LIFT ANGLE (FULLY ATTACHED FLOW)

$$\frac{\tau_0 \cos \Gamma}{\delta/2}$$

$$\frac{h_0/c}{1+h_0/c}$$

FIG 5
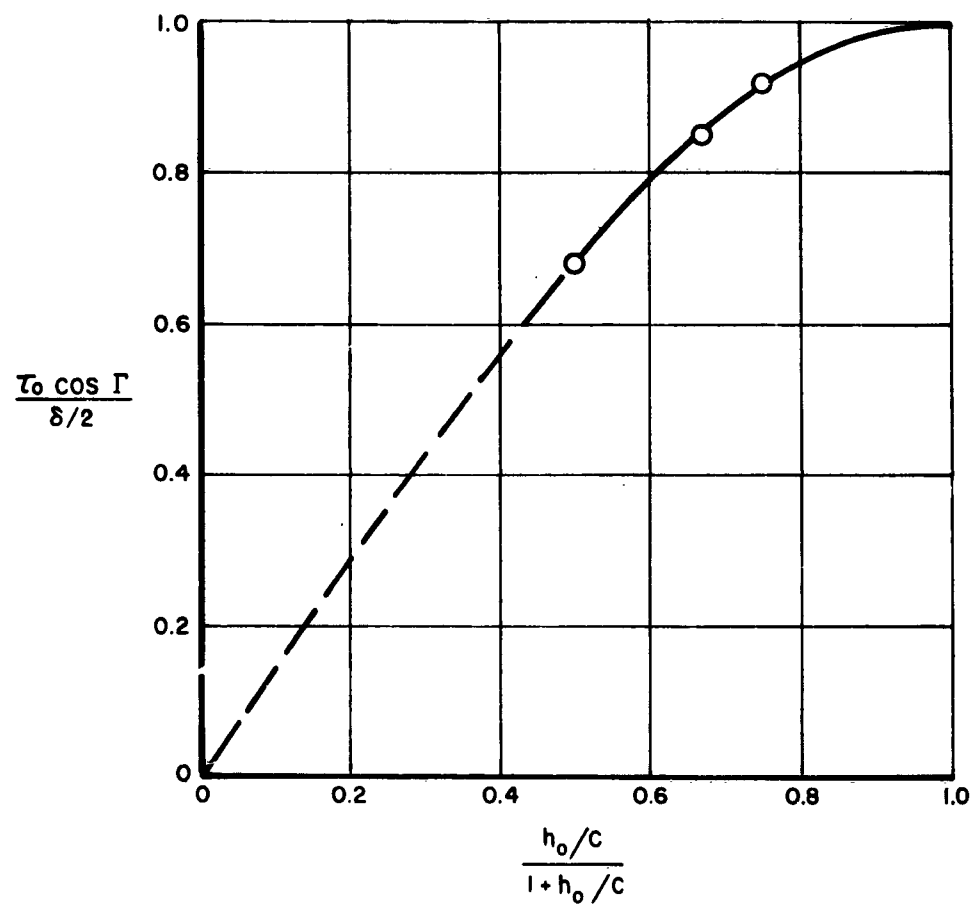
VENTILATION BOUNDARIES AND FLOW PHOTOGRAPHS

FIG 6
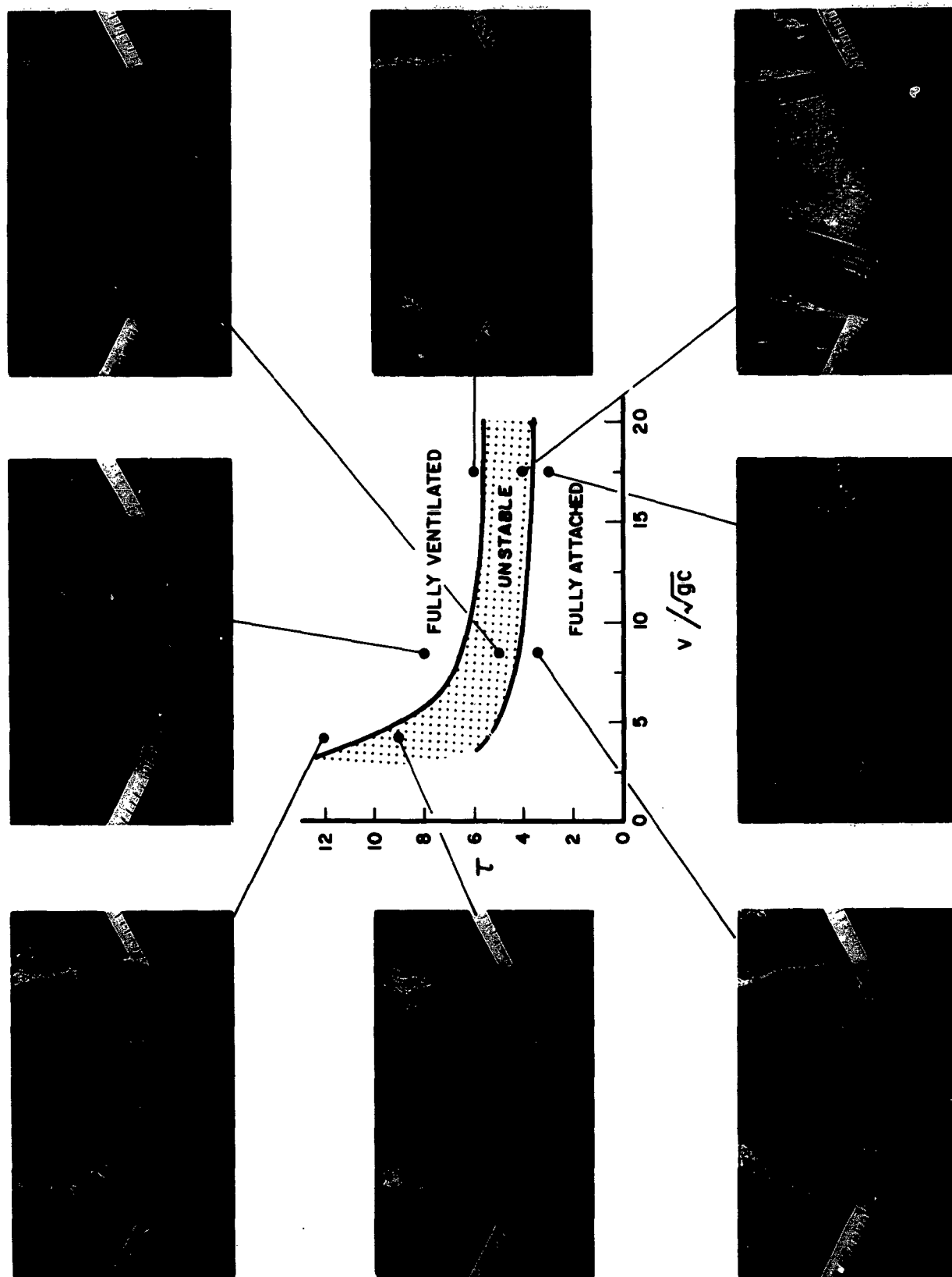
DESIGN CHART FOR STABLE OPERATION

FIG 6a. LIFT CHARACTERISTICS

FULLY ATTACHED

FULLY VENTILATED

C_L^I

τ COS Γ (DEG.)

FIG 6b. VENTILATION BOUNDARIES

FULLY ATTACHED

UNSTABLE

FULLY VENTILATED

$\dfrac{V}{\sqrt{gc}}$

τ COS Γ (DEG.)
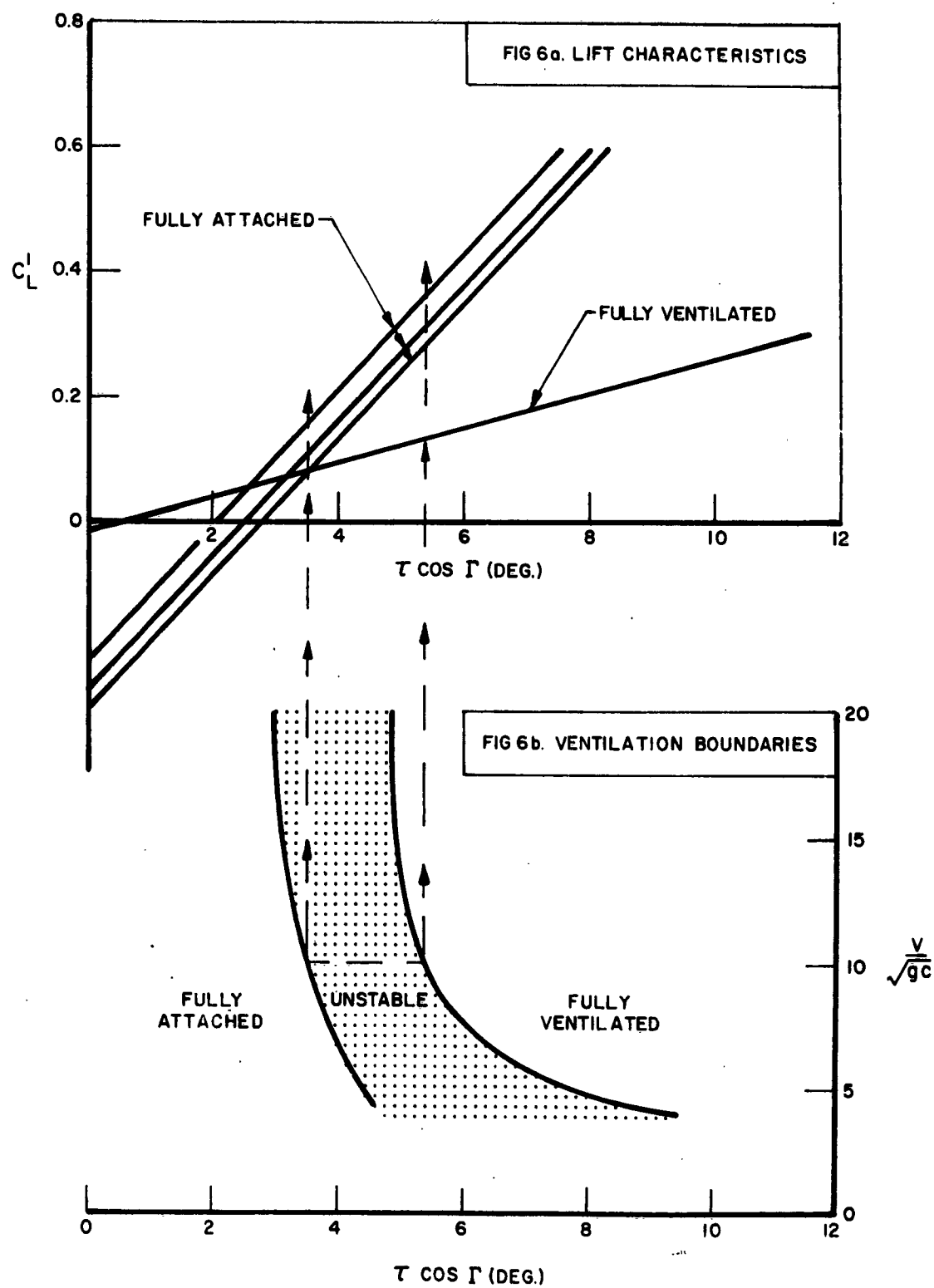
DISTRIBUTION LIST

Chief of Naval Research
Department of the Navy
Washington 25, D.C.
Attn: Codes 438   3
          461   1
          463   1
          466   1

Commanding Officer
Office of Naval Research
Branch Office
495 Summer Street
Boston 10, Massachusetts   1

Commanding Officer
Office of Naval Research
Branch Office
346 Broadway
New York 13, New York   1

Commanding Officer
Office of Naval Research
Branch Office
1030 East Green Street
Pasadena, California   1

Commanding Officer
Office of Naval Research
Branch Office
1000 Geary Street
San Francisco 9, Calif.   1

Commanding Officer
Office of Naval Research
Branch Office
Navy #100, Fleet Post Office
New York, New York   25

Director, Naval Research Lab
Washington 25, D. C.
Attn: Code 2027   6

Chief, Bureau of Naval Weapons
Department of the Navy
Washington 25, D. C.
Attn: Codes RUAW-4   1
          RRRE   1
          RAAD   1
          RAAD-222   1
          DIS-42   1

Chief, Bureau of Ships
Department of the Navy
Washington 25, D. C.
Attn: Codes 106   1
          310   1
          312   1
          335   1
          420   1
          421   1
          440   1
          442   1
          449   1

Chief, Bureau of Yards and Docks
Department of the Navy
Washington 25, D. C.
Attn: Code D-400   1

Commanding Officer and Director
David Taylor Model Basin
Washington 7, D. C.
Attn: Codes 108   1
          142   1
          500   1
          513   1
          520   1
          526   1
          526A   1
          530   1
          533   1
          580   1
          585   1
          589   1
          591   1
          591A   1
          700   1

Commander, U. S. Naval Ordnance
Test Station
China Lake, California
Attn: Code 753   1

Commander, U. S. Naval Ordnance
Test Station
Pasadena Annex
3202 E. Foothill Blvd.
Pasadena 8, California   1
Attn: Code P-508   1

Commander, Planning Dept.
Portsmouth Naval Shipyard
Portsmouth, New Hampshire   1

Commander, Planning Dept.
Boston Naval Shipyard
Boston 29, Massachusetts   1

Commander, Planning Dept.
Pearl Harbor Naval Shipyard
Navy #128, Fleet Post Office
San Francisco, California   1

Commander, Planning Dept.
San Francisco Naval Shipyard
San Francisco 24, Calif.   1

Commander, Planning Dept.
Mare Island Naval Shipyard
Vallejo, California   1

Commander, Planning Dept.
New York Naval Shipyard
Brooklyn 1, New York   1

Commander, Planning Dept.
Puget Sound Naval Shipyard
Bremerton, Washington   1

Commander, Planning Dept.
Philadelphia Naval Shipyard
U. S. Naval Base
Philadelphia 12, Penna.   1

Commander, Planning Dept.
Norfolk Naval Shipyard
Portsmouth, Virginia   1

Commander, Planning Dept.
Charleston Naval Shipyard
U. S. Naval Base
Charleston, South Carolina   1

Commander, Planning Dept.
Long Beach Naval Shipyard
Long Beach 2, California   1

Commander, Planning Dept.
U. S. Naval Weapons Lab
Dahlgren, Virginia   1

Commander, U. S. Naval
Ordnance Laboratory
White Oak, Maryland   1

Dr. A. V. Hershey
Computation and Exterior
  Ballistics Laboratory
U. S. Naval Weapons Lab
Dahlgren, Virginia   1

Superintendent, U. S. Naval
Academy
Annapolis, Maryland
Attn: Library   1

Superintendent
U. S. Naval Postgraduate School
Monterey, California   1

Commandant
U. S. Coast Guard
1300 E Street, N.W.
Washington, D. C.   1

Secretary Ship Structure Comm.
U. S. Coast Guard Headquarters
1300 E Street, N. W.
Washington, D. C.   1

Commander
Military Sea Trans. Service
Department of the Navy
Washington 25, D. C.   1

U. S. Maritime Administration
GAO Building
441 G Street, N. W.
Washington, D. C.
Attn: Div. of Ship Design   1
       Div. of Research   1
       Mr. R. P. Godwin   1

Superintendent
U. S. Merchant Marine Academy
Kings Point, Long Island, N.Y.
Attn: Capt. L. S. McCready   1
          (Dept. of Engineering)

Commanding Officer and Director
U. S. Navy Mine Defense Lab
Panama City, Florida   1

Commanding Officer, NROTC and
Naval Administrative Unit
Mass. Inst. of Technology
Cambridge 39, Massachusetts   1

U. S. Army Trans. Research and
Development Command
Fort Eustis, Virginia
Attn: Marine Transport Div.   2

Director of Research
National Aeronautics and Space
Administration
1512 H Street, N. W.
Washington 25, D. C.   1

New York University
Inst. of Mathematical Sciences
25 Waverly Place
New York 3, New York
Attn: Professor J. Keller   1
        Professor J. J. Stoker   1
        Professor R. Kraichnan   1

The John Hopkins University
Dept. of Mechanical Engr.
Baltimore 18, Maryland
Attn: Prof. S. Corrsin   1
        Prof. O. N. Phillips   2

Mass. Inst. of Technology
Dept. of Naval Architecture
and Marine Engineering
Cambridge 39, Massachusetts
Attn: Prof. M. A. Abkowitz   1

Dr. G. F. Wislicenus
Ordnance Research Laboratory
Pennsylvania State University
University Park, Pennsylvania   1
Attn: Dr. M. Sevik   1

Professor R. C. DiPrima
Dept. of Mathematics
Rensselaer Polytechnic Inst.
Troy, New York   1

Webb Inst. of Naval Arch.
Crescent Beach Road
Glen Cove, New York
Attn: Technical Library   1

Director
Woods Hole Oceanographic Inst.
Woods Hole, Massachusetts   1

Commander, Air Research and
Development Command
Air Force Office of Scientific
 Research
14th and Constitution
Washington 25, D. C.
Attn: Mechanics Branch   1

Commander, Wright Air Develop-
ment Division
Aircraft Laboratory
Wright-Patterson Air Force
Base, Ohio
Attn: Mr. W. Mykytow,
Dynamics Branch   1

Cornell Aeronautical Lab
4455 Genesee Street
Buffalo, New York
Attn: Mr. W. Tangoff   1
        Mr. R. White   1

Mass. Inst. of Technology
Fluid Dynamics Research Lab
Cambridge 39, Mass.
Attn: Prof. H. Ashley   1
        Prof. M. Landahl   1
        Prof. J. Dugundji   1

Hamburgische Schiffbau-
  Versuchsanstalt
Bramfelder Strasse 164
Hamburg 33, Germany
Attn: Dr. O. Grim   1
        Dr. H. W. Lerbs   1

Inst. für Schiffbau der
Universitas Hamburg
Berliner Ter 21
Hamburg 1, Germany
Attn: Prof. G. P. Weinblum   1

Max-Planck Institut für
Strömungsforschung
Bottingerstrasse 6/8
Gottingen, Germany
Attn: Dr. H. Reichardt   1

Hydro-og Aerodynamisk
Laboratorium
Lyngby, Denmark
Attn: Prof. Carl Prohaska   1

Skipsmodelltanken
Trondheim, Norway
Attn: Prof. J. K. Lunde   1

Versuchsanstalt für Wasserbau
und Schiffbau
Schleuseninsel im Tiergarten
Berlin, Germany
Attn: Dr. S. Schuster   1

Technische Hogeschool
Institut voor Toogapaste
Wiskunde
Julianalaan 132
Delft, Netherlands
Attn: Prof. R. Timman   1

Bureau D'Analyse et de
Techerche Appliquees
2 Rue Joseph Sansboeuf
Paris 8, France
Attn: Prof. L. Malavard   1

Netherlands Ship Model Basin
Wageningen, Netherlands
Attn: Dr. Ir.J.D. van Manen 1

Allied Research Assoc., Inc.
43 Leon Street
Boston 15, Massachusetts
Attn: Dr. T. R. Goodman   1

National Physical Lab
Teddington, Middlesex, England
Attn: Dr. F. H. Todd, Supt.
Ship Division   1
Head Aerodynamics Div.   1
Mr. A. Silverleaf   1

Head, Aerodynamics Dept.
Royal Aircraft Establishment
Farnborough, Hants, England
Attn: Mr. M. O. W. Wolfe   2

Boeing Airplane Co.
Seattle Division
Seattle, Washington
Attn: Mr. M. J. Turner   1

Electric Boat Division
General Dynamics Corp.
Groton, Connecticut
Attn: Mr. R. McCandliss   1

General Applied Sciences Labs,
Inc.
Merrick and Stewart Avenues
Westbury, Long Island, N. Y. 1

Gibbs and Cox, Inc.
21 West Street
New York, N. Y.   1

Grumman Aircraft Eng. Corp.
Bethpage, Long Island, N. Y.
Attn: Mr. E. Baird   1
        Mr. E. Bower   1

Grumman Aircraft Eng. Corp.
Dynamic Developments Div.
Babylon, New York   1

Lockheed Aircraft Corp.
Missiles and Space Div.
Palo Alto, California
Attn: R. W. Kermeen   1

Midwest Research Inst.
425 Volker Blvd.
Kansas City 10, Missouri
Attn: Mr. Zeydel   1

Director, Dept. of Mechanical
Sciences
Southwest Research Inst.
8500 Culebra Road
San Antonio 6, Texas
Attn: Dr. H.N. Abramson   1
        Mr. G. Ransleben   1
        Editor, Applied
          Mechanics Review   1

Convair
A Div. of General Dynamics
San Diego, California
Attn: Mr. R.H. Oversmith   1
        Mr. A.D. MacLellan   1
        Mr. H.T. Brooke   1

Dynamic Developments, Inc.
15 Berry Hill Road
Oyster Bay, Long Island, N.Y. 1

Dr. S. F. Hoerner
148 Busteed Drive
Midland Park, N. J.   1

Hydronautics, Inc.
200 Monroe Street
Rockville, Maryland
Attn: Mr. Phillip Eisenberg 1

Rand Development Corp.
13600 Deise Avenue
Cleveland 10, Ohio
Attn: Dr. A. S. Iberall   1

U. S. Rubber Company
Research and Development Dept.
Wayne, New Jersey
Attn: Mr. L. M. White   1

Technical Research Group, Inc.
2 Aerial Way
Syosset, Long Island, N.Y.
Attn: Dr. Jack Kotik   1

Director, Langley Research Ctr.
Langley Field Virginia
Attn: Mr. J. B. Parkinson   2
         Mr. I. E. Garrick   1
         Mr. D. J. Marten   1

Director
Engineering Sciences Division
National Science Foundation
1951 Constitution Ave., N. W.
Washington 25, D. C.   1

Director
National Bureau of Standards
Washington 25, D. C.
Attn: Fluid Mechanics Div.
         (Dr. G. B. Schubauer) 1
         Dr. G. H. Keulegan   1
         Dr. J. M. Franklin   1

Armed Services Technical
Information Agency
Arlington Hall Station
Arlington 12., Virginia   10

Office of Technical Services
Department of Commerce
Washington 25, D. C.   1

California Institute of
Technology
Pasadena 4, California
Attn: Prof. M. S. Plesset   1
         Prof. T. Y. Wu   1
         Prof. A. J. Acosta   1

University of California
Department of Engineering
Los Angeles 24, California
Attn: Dr. A. Powell   1

Director, Scripps Institute
of Oceanography
University of California
La Jolla, California   1

Professor M. L. Albertson
Dept. of Civil Engineering
Colorado A&M College
Fort Collins, Colorado   1

Professor J. E. Cermak
Dept. of Civil Engineering
Colorado State University
Fort Collins, Colorado   1

Professor W. R. Sears
Graduate School of
Aeronautical Engineering
Cornell University
Ithaca, New York   1

State University of Iowa
Iowa Inst. of Hydraulic
Research
Iowa City, Iowa
Attn: Dr. H. Rouse   1
         Dr. L. Landweber   1

Harvard University
Cambridge 38, Massachusetts
Attn: Prof. G. Birkhoff
         (Dept. of Math.)   1
         Prof. G. F. Carrier
         (Dept. of Math.)   1

Massachusetts Inst. of Tech.
Cambridge 39, Mass.
Attn: Dept. of Naval Archi-
         tecture and Marine Engr.1
         Prof. A. T. Ippen   1

University of Michigan
Ann Arbor, Michigan
Attn: Prof. R. B. Couch
         (Dept. of Naval Arch.) 1
         Prof. W. W. Willmarth
         (Aero. Engr. Dept.)   1
         Prof. M. S. Uberoi
         (Aero. Engr. Dept.)   1

Dr. L. G. Straub, Director
St. Anthony Falls Hydraulic
 Lab
University of Minnesota
Minneapolis 14, Minnesota   1
Attn: Mr. Wetzel   1
         Prof. B. Silberman   1

Professor J. J. Foody
Engineering Dept. New York
State University Maritime
College
Fort Schulyer, New York   1

Mr. C. Wigley
Flat 102
6-9 Charterhouse Square
London, E. C. 1, England   1

Avco Corporation
Lycoming Division
1701 K Street, N. W.
Apt. #904
Washington, D. C.
Attn: Mr. T. A. Duncan   1

Mr. J. G. Baker
Baker Manufacturing Company
Evansville, Wisconsin   1

Curtiss-Wright Corporation
Research Division
Turbomachinery Division
Quehanna, Pennsylvania   ?
Attn: Mr. George H. Pedersen

Hughes Tool Company
Aircraft Division
Culver City, California
Attn: Mr. M. S. Harned   1

Lockheed Aircraft Corp.
California Division
Hydrodynamics Research
Burbank, California
Attn: Mr. Kenneth E. Hodge   1

National Research Council
Montreal Road
Ottawa 2, Canada
Attn: Mr. E. S. Turner   1

The Rand Corporation
1700 Main Street
Santa Monica, California
Attn: Dr. Blaine Parkin   1

Stanford University
Dept. of Civil Engineering
Stanford, California
Attn: Dr. Byrne Perry   1
        Dr. E. Y. Hsu   1

Waste King Corporation
5550 Harbor Street
Los Angeles 22, California
Attn: Dr. A. Schneider   1

Mr. David Wellinger
Hydrofoil Projects
Radio Corporation of America
Burlington, Massachusetts   1

Versuchsanstalt für Wasserbau
und Schiffbau
Schleuseninsel im Tiergarten
Berlin, Germany
Attn: Dr. Grosse   1
        Dr. H. Schwanecke   1

DAVIDSON LABORATORY Report 952

VENTILATION INCEPTION ON A SURFACE-PIERCING
DIHEDRAL HYDROFOIL WITH PLANE-FACE WEDGE SECTION
by Gerard Fridsma, October 1963. Prepared for
Office of Naval Research, Contract Nonr 263(20),
D.L. Project 2080
iv + 19 pages, 6 figures   UNCLASSIFIED

   A surface-piercing, dihedral hydrofoil was
tested to investigate the inception and extent of
ventilation. The foil of wedge-shaped cross-section
and dihedral angle of 30 degrees was shown to venti-
late under a number of operating conditions when the
                                        (see over)

DAVIDSON LABORATORY Report 952

VENTILATION INCEPTION ON A SURFACE-PIERCING
DIHEDRAL HYDROFOIL WITH PLANE-FACE WEDGE SECTION
by Gerard Fridsma, October 1963. Prepared for
Office of Naval Research, Contract Nonr 263(20),
D.L. Project 2080
iv + 19 pages, 6 figures   UNCLASSIFIED

   A surface-piercing, dihedral hydrofoil was
tested to investigate the inception and extent of
ventilation. The foil of wedge-shaped cross-section
and dihedral angle of 30 degrees was shown to venti-
late under a number of operating conditions when the
                                        (see over)

DAVIDSON LABORATORY Report 952

VENTILATION INCEPTION ON A SURFACE-PIERCING
DIHEDRAL HYDROFOIL WITH PLANE-FACE WEDGE SECTION
by Gerard Fridsma, October 1963. Prepared for
Office of Naval Research, Contract Nonr 263(20),
D.L. Project 2080
iv + 19 pages, 6 figures   UNCLASSIFIED

   A surface-piercing, dihedral hydrofoil was
tested to investigate the inception and extent of
ventilation. The foil of wedge-shaped cross-section
and dihedral angle of 30 degrees was shown to venti-
late under a number of operating conditions when the
                                        (see over)

DAVIDSON LABORATORY Report 952

VENTILATION INCEPTION ON A SURFACE-PIERCING
DIHEDRAL HYDROFOIL WITH PLANE-FACE WEDGE SECTION
by Gerard Fridsma, October 1963. Prepared for
Office of Naval Research, Contract Nonr 263(20),
D.L. Project 2080
iv + 19 pages, 6 figures   UNCLASSIFIED

   A surface-piercing, dihedral hydrofoil was
tested to investigate the inception and extent of
ventilation. The foil of wedge-shaped cross-section
and dihedral angle of 30 degrees was shown to venti-
late under a number of operating conditions when the
                                        (see over)

speed, draft, and angle of attack were varied. Stable regions of fully attached and fully ventilated flow are defined by ventilation inception boundaries which are shown to depend on the speed and angle of attack and not on the depth of submergence. Expressions for the forces experienced by the foil under these stable flow conditions are derived and are shown to be in good agreement with the experimental results.

speed, draft, and angle of attack were varied. Stable regions of fully attached and fully ventilated flow are defined by ventilation inception boundaries which are shown to depend on the speed and angle of attack and not on the depth of submergence. Expressions for the forces experienced by the foil under these stable flow conditions are derived and are shown to be in good agreement with the experimental results.

speed, draft, and angle of attack were varied. Stable regions of fully attached and fully ventilated flow are defined by ventilation inception boundaries which are shown to depend on the speed and angle of attack and not on the depth of submergence. Expressions for the forces experienced by the foil under these stable flow conditions are derived and are shown to be in good agreement with the experimental results.

speed, draft, and angle of attack were varied. Stable regions of fully attached and fully ventilated flow are defined by ventilation inception boundaries which are shown to depend on the speed and angle of attack and not on the depth of submergence. Expressions for the forces experienced by the foil under these stable flow conditions are derived and are shown to be in good agreement with the experimental results.